1. TENSORIAL ASPECTS OF PHYSICAL PROPERTIES

Table 1.7.5.1. *Mineral nonlinear crystals*

The letters (*a*, *b*, *c*) refer to the crystallographic frame. These data are mainly extracted from Bordui & Fejer (1993).

(*a*) SHG (1.064–0.532 μm).

	KD_2PO_4 (KD*P)	$NH_4H_2PO_4$ (ADP)	CsD_2AsO_4 (CD*A)	β-BaB_2O_4 (BBO)	LiB_3O_5 (LBO)
Crystal class	$\bar{4}2m$	$\bar{4}2m$	$\bar{4}2m$	$3m$	$mm2$
Transparency (μm)	0.18–1.8	0.184–1.5	0.27–1.66	0.198–2.6	0.16–2.3
Non-critical λ_{pump} at room temperature (μm)					
Type I	0.519	0.524	1.045	0.409	0.554 (*c*) 1.212 (*a*)
Type II	—	—	—	—	1.19 (*b*)
T_{pm} (K)			385		421
Type of phase matching	II	II	I	I	I (*a*)
θ (°)	54	62	90	23	90
φ (°)	—	—	—	—	0
Effective coefficient d_{eff} (pm V^{-1})	0.35	0.39	0.30	1.9	0.85
Angular bandwidth (mrad cm)	2.3	2.2	51	0.53	72
Walk-off angles					
ρ^{ω} (°)	1.3	1.2	0	0	0
$\rho^{2\omega}$ (°)	1.4	1.5	0	3.2	0
Thermal bandwidth (K cm)	12	2.1	3.3	51	3.9
Spectral bandwidth (nm cm)	5.6	26	2.5	2	3.6
Surface optical damage threshold (GW cm^{-2})	5 (1 ns) >8 (0.6 ns at 0.53 μm)	6 (15 ns) >8 (0.6 ns at 0.53 μm)	0.25 (12 ns)	13.5 (1 ns) 23 (14 ns) 32 (8 ns at 0.53 μm)	25 (0.1 ns) 1.4 (12 ns at 0.78 μm)

SHG (1.064–0.532 μm) (*cont.*).

	$KTiOPO_4$ (KTP)	$KNbO_3$	5% MgO:$LiNbO_3$	$LiIO_3$
Crystal class	$mm2$	$mm2$	$3m$	$6mm$
Transparency (μm)	0.35–4.5	0.4–5.5	0.35–5	0.31–5 || to **c**, 0.34–4 ⊥ to **c**
Non-critical λ_{pump} at room temperature (μm)				
Type I	—	0.860 (*a*) 0.982 (*b*)		0.756
Type II	0.990 (*b*) 1.081 (*a*)	—		—
T_{pm} (K)		456	380	
Type of phase matching	II (*a*, *b*)	I (*b*)	I	I
θ (°)	90	90	90	30
φ (°)	23	90	—	—
Effective coefficient d_{eff} (pm V^{-1})	2.4	−13	4.7	1.8
Angular bandwidth (mrad cm)	9	13	33	0.34
Walk-off angles				
ρ^{ω} (°)	0.20	0	0	0
$\rho^{2\omega}$ (°)	0.27	0	0	4.3
Thermal bandwidth (K cm)	17	0.3	0.75	23
Spectral bandwidth (nm cm)	0.46	0.12	0.31	0.82
Surface optical damage threshold (GW cm^{-2})	9–20 (1 ns) >2 (10 ns at 0.5 μm)	7 (1 ns) >1 (10 ns)		2 (1 ns) 1 (0.1 ns at 0.53 μm)

(*b*) SHG (532–266 nm).

	KD_2PO_4 (KD*P)	$NH_4H_2PO_4$ (ADP)	β-BaB_2O_4 (BBO)
Crystal class	$\bar{4}2m$	$\bar{4}2m$	$\bar{4}2m$
Transparency (μm)	0.18–1.8	0.184–1.5	0.198–2.6
Non-critical λ_{pump} at room temperature (μm)	0.519	0.524	0.409
T_{pm} (K)	308	324	
Type of phase matching	I	I	I
θ (°)	90	90	47
φ (°)	—	—	—
Effective coefficient d_{eff} (pm V^{-1})	0.44	0.57	2.0
Angular bandwidth (mrad cm)	16	16	0.16
Walk-off angles			
ρ^{ω} (°)	0	0	0
$\rho^{2\omega}$ (°)	0	0	4.8
Thermal bandwidth (K cm)	3.0	0.54	4.0
Spectral bandwidth (nm cm)	0.13	0.13	0.073
Surface optical damage threshold (GW cm^{-2})	5 (1 ns) >8 (0.6 ns at 0.53 μm)	6 (15 ns) >8 (0.6 ns at 0.53 μm)	13.5 (1 ns) 23 (14 ns) 32 (8 ns at 0.53 μm)

Table 1.7.5.1 (*cont.*)

(*c*) SHG (4000–2000 nm).

	$AgGaS_2$	$AgGaSe_2$	$ZnGeP_2$	Tl_3AsSe_3 (TAS)
Crystal class	$\bar{4}2m$	$\bar{4}2m$	$\bar{4}2m$	$3m$
Transparency (μm)	0.5–13	0.78–18	0.74–12	1.3–17
Non-critical λ_{pump} at room temperature (μm)	1.8 and 11.2	3.1 12.8	3.2 10.3	—
Type of phase matching	I	I	I	I
θ (°)	31	52	56	33
φ (°)	—	—	—	—
Effective coefficient d_{eff} (pm V^{-1})	10.4	28	70	68
Angular bandwidth (mrad cm)	3.7	6.0	5.0	4.2
Walk-off angles				
ρ^{ω} (°)	0	0	0.65	0
$\rho^{2\omega}$ (°)	1.2	0.64	0	3.1
Thermal bandwidth (K cm)	50	50	40	5.7 (SHG at 10.6 μm)
Spectral bandwidth (nm cm)	11	22	20	—
Surface optical damage threshold (GW cm^{-2})	0.5 (10 ns bulk)	0.01–0.04 (50 ns, 2 μm) 0.02–0.03 (10 ns at 10.6 μm)	0.05 (25 ns at 2 μm) 1 (2 ns at 10.6 μm)	0.016 (250 ns at 10.6 μm)

exists even if the refractive indices do not vary with the direction of propagation, which would be the case for an interaction involving only ordinary waves during the rotation. The most general expression of the generated harmonic power, *i.e.* $P^{n\omega}(\alpha) = j(\alpha)\sin^2\Psi(\alpha)$, must take into account the angular dependence of all the refractive indices, in particular for the calculation of the coherence length and transmission coefficients (Herman & Hayden, 1995). The effective coefficient is then deduced from the angular spacing of the Maker fringes and from the conversion efficiency at the maxima of oscillation.

A continuous variation of the phase mismatch can also be performed by translating a wedged sample as shown in Fig. 1.7.4.1(*b*) (Perry, 1991). The harmonic power oscillates as a function of the displacement x. In this case, the interacting waves stay collinear and the oscillation is only caused by the variation of the crystal length. Relation (1.7.4.2) is then valid, by considering a variable crystal length $L(x) = x\tan\beta$; $A^{n\omega}$ and $l_c^{n\omega}$ are constant. The space between two maxima of the wedge fringes is $\Delta x_c = 2l_c/\tan\beta$, which allows the determination of l_c. Then the measurement of the harmonic power, $P_{max}^{n\omega}$, generated at a maximum leads to the absolute value of the effective coefficient:

$$|d_{eff}^{n\omega}| = \left\{\frac{P_{max}^{n\omega}}{A^{n\omega}[P^{\omega}(0)]^2 l_c^2}\right\}^{1/2}$$
$$l_c = (\Delta x_c \tan\beta/2). \qquad (1.7.4.3)$$

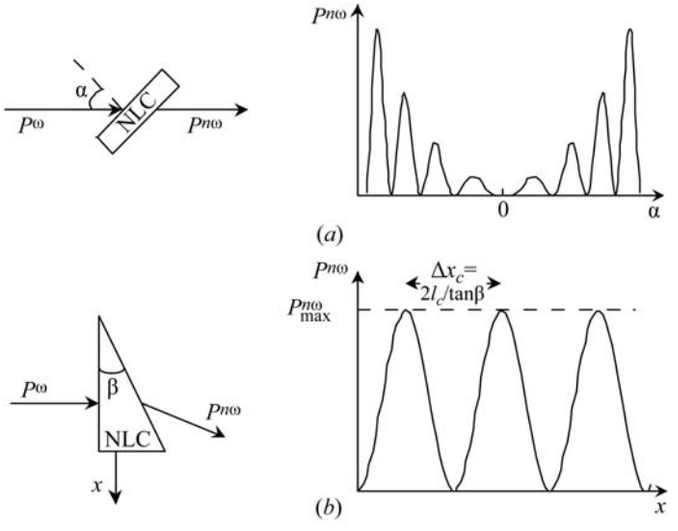

Fig. 1.7.4.1. (*a*) The Maker-fringes technique; (*b*) the wedge-fringes technique.

It is necessary to take into account a multiple reflection factor in the expression of $A^{n\omega}$.

The Maker-fringes and wedge-fringes techniques are essentially used for relative measurements referenced to a standard, usually KH_2PO_4 (KDP) or quartz (α-SiO_2).

1.7.4.2.2. *Phase-matched interaction method*

The use of phase-matched interactions is suitable for absolute and accurate measurements (Eckardt & Byer, 1991; Boulanger, Fève *et al.*, 1994). The sample studied is usually a slab cut in a phase-matching direction. The effective coefficient is determined from the measurement of the conversion efficiency using the theoretical expressions given by (1.7.3.30) and (1.7.3.42) for SHG, and by (1.7.3.80) for THG, according to the validity of the corresponding approximations. Because of phase matching, the generated harmonic power is not weak and it is measurable with very good accuracy, even with a c.w. conversion efficiency.

Recent experiments have been performed in a KTP crystal cut as a sphere (Boulanger *et al.*, 1997, 1998): the absolute magnitudes of the quadratic effective coefficients are measured with an accuracy of 10%, which is comparable with typical experiments on a slab.

For both non-phase-matched and phase-matched techniques, it is important to know the refractive indices and to characterize the spatial, temporal and spectral properties of the pump beam carefully. The considerations developed in Section 1.7.3 about effective coefficients and field tensors allow judicious choices of configurations of polarization and directions of propagation for the determination of the absolute value and relative sign of the independent coefficients of tensors $\chi^{(2)}$ and $\chi^{(3)}$, given in Tables 1.7.2.2 to 1.7.2.5 for the different crystal point groups.

1.7.5. The main nonlinear crystals

Tables 1.7.5.1 and 1.7.5.2 give some characteristics of the main nonlinear crystals. No single nonlinear crystal is the best for all applications, so the different materials must be seen as complementary to each other.

A complete review of mineral crystals is given in Bordui & Fejer (1993). General references for organic crystals may be found, for example, in Chemla & Zyss (1987), Zyss (1994), and Dmitriev *et al.* (1991). Perry (1991) deals with both organic and inorganic materials.

A new generation of materials has been developed since 1995 for the design of new compact all-solid-state laser sources. These optical materials are multifunction crystals, such as $LiNbO_3$:Nd^{3+}, $Ba_2NaNb_5O_{15}$:Nd^{3+}, $CaGd_4(BO_3)_3O$:Nd^{3+} or $YAl_3(BO_3)_4$:Yb^{3+}, for example, in which the laser effect and the nonlinear frequency